MOLECULAR AND CELLULAR BIOLOGY, Sept. 2002, p. 6363–6374 Vol. 22, No. 18
0270-7306/02/$04.00+0 DOI: 10.1128/MCB.22.18.6363–6374.2002

Fer Kinase Is Required for Sustained p38 Kinase Activation and Maximal Chemotaxis of Activated Mast Cells

Andrew W. B. Craig[1] and Peter A. Greer[1,2,3]*

Department of Biochemistry,[1] Department of Pathology,[2] and Division of Cancer Biology and Genetics,[3] Queen's University Cancer Research Institute, Queen's University, Kingston, Ontario, Canada K7L 3N6

Received 20 May 2002/Returned for modification 4 June 2002/Accepted 12 June 2002

Mast cells play important roles in inflammation and immunity and express the high-affinity immunoglobulin E receptor (FcεRI) and the receptor protein-tyrosine kinase Kit. Aggregation of FcεRI via antigen binding elicits signals leading to the release of preformed inflammatory mediators as well as de novo-synthesized lipid mediators and cytokines and to elevated cell adhesion and migration. Here, we report that in mouse bone marrow-derived mast cells, Fer kinase is activated downstream of activated FcεRI and activated Kit receptor, and this activation is abolished in cells homozygous for a kinase-inactivating mutation in Fer (*fer*$^{DR/DR}$). Interestingly, the highly related Fps/Fes kinase is also activated upon FcεRI aggregation. This report represents the first description of a common signaling pathway activating Fer and Fps/Fes. While Fer-deficient cells showed similar activation of the Erk mitogen-activated protein (MAP) kinases, p38 MAP kinase activation was less sustained than that in wild-type cells. Although no major defects were observed in degranulation, leukotriene biosynthesis, and cytokine secretion, Fer-deficient cells displayed increased adhesion and decreased motility upon activation of FcεRI and the Kit receptor. The restoration of Fer kinase activity in *fer*$^{DR/DR}$ mast cells resulted in prolonged p38 kinase activation and increased antigen-mediated cell migration of sensitized mast cells. Thus, Fer is required for maximal p38 kinase activation to promote the chemotaxis of activated mast cells. Further studies with mast cells derived from *fps*/*fes*-deficient mice will be required to provide insight into the role of Fps/Fes in mast cell activation.

Mast cells are bone marrow-derived granulocytes that reside close to blood vessels and peripheral nerves and below epithelial cell surfaces exposed to external environments, including the respiratory and gastrointestinal tracts and skin (1, 62). While mast cell activation can cause allergic reactions and potentially life-threatening anaphylaxis, these cells also play a critical protective function against infection by parasites and bacteria (17, 40). Mast cells and basophils, which are highly related cells that circulate in the bloodstream, have cytoplasms full of granules containing preformed mediators, including histamine, serotonin, heparin, tryptases, and other enzymes that, upon release, cause rapid changes in the surrounding tissues via changes in vascular permeability, growth factor activity, and remodeling of the extracellular matrix (62). In addition, activated mast cells also synthesize and secrete lipid mediators, including leukotrienes and prostaglandins, which are products of the lipooxygenase and cyclooxygenase pathways, respectively. The major leukotriene produced by mast cells is leukotriene C_4 (LTC_4); upon release, LTC_4 is converted to LTD_4 and LTE_4, leading to prolonged bronchoconstriction, increased bronchial mucus production, increased venular permeability and arterial constriction, and cutaneous wheal-and-flare responses. The secretion of prostaglandin D_2 by activated mast cells inhibits platelet aggregation and promotes the recruitment of neutrophils (40). Mast cells are also a rich source of cytokines, including interleukin 2 (IL-2), IL-3, IL-4, IL-5, IL-6, IL-10, IL-13, gamma interferon, tumor necrosis factor alpha (TNF-α), and granulocyte-monocyte colony-stimulating factor, and of chemokines, such as monocyte chemoattractant protein 1 and macrophage inhibitory proteins 1α and 1β. The secretion of these factors at later times after mast cell activation leads to changes in the growth, activation, and motility of leukocytes and lymphocytes (62).

Mast cells and basophils play a role in immune surveillance and can recognize antigens via cell-associated immunoglobulin E (IgE) bound to its high-affinity receptor (FcεRI). FcεRI is composed of a predominantly extracellular α chain that binds the Fc portion of IgE, a tetramembrane-spanning β subunit, and a dimeric γ chain. The β and γ chains possess important signaling motifs that are composed of twice-repeated YxxL sequences flanking seven variable residues and that are called immunoreceptor tyrosine-based activation motifs (ITAMs) (12). ITAMs are also found in the B-cell antigen receptor, T-cell receptor signaling subunits (46), and the glycoproteinVI (GPVI) receptor for collagen on platelets (61). Upon activation, these receptors are recruited to specialized cholesterol-rich regions of the plasma membrane that are called lipid rafts (also called glycolipid-enriched membrane domains or detergent-resistant membranes) and that allow for the compartmentalization of proteins involved in signaling and receptor endocytosis (22). Signaling from FcεRI ITAMs is initiated by the Src family protein-tyrosine kinase (PTK) Lyn, which interacts with the FcεRI β chain independent of its phosphorylation status (60). The aggregation of FcεRI by multivalent antigens leads to Lyn autophosphorylation in *trans* and to the subsequent phosphorylation of ITAM tyrosine residues. These steps provide high-affinity docking sites on γ chains for the dual Src homology 2 domain-containing kinase Syk, which is activated upon phosphorylation by Lyn (48). Syk then propagates signals

* Corresponding author. Mailing address: Cancer Research Labs, Rm. A309, Botterell Hall, Queen's University, Kingston, Ontario, Canada K7L 3N6. Phone: (613) 533-2813. Fax: (613) 533-6830. E-mail: greerp@post.queensu.ca.

leading to increased lipid metabolism via activation of the Ras mitogen-activated protein (MAP) kinase pathway (28), degranulation via phospholipase C-γ- and protein kinase C-induced calcium mobilization (9), and cytokine expression through the activation of a number of transcription factors, including nuclear factor of activated T cells (24) and AP-1 (14, 44). It was recently shown that the binding of monomeric IgE to FcεRI is sufficient to generate a survival signal and induce cytokine gene expression (4, 30). However, the aggregation of FcεRI is required for degranulation and release of lipid mediators. Mast cell activation downstream of either FcεRI or the Kit receptor also leads to increased cell adhesion (13, 53) and increased cell motility (54, 64). The activation of p38 MAP kinase is critical for both antigen-dependent mast cell migration via FcεRI (27) and chemotaxis upon Kit receptor activation (59).

Activation of the nonreceptor PTK Fer upon FcεRI aggregation was demonstrated previously with an immortalized mast cell line (42). Fer and the highly related Fps/Fes (hereafter referred to as Fps) PTKs make up a unique subfamily of PTKs (52). These kinases possess an N-terminal domain containing three predicted coiled-coil domains that mediate trimerization (7, 11, 33, 45), followed by a Src homology 2 domain and a C-terminal kinase domain. Also, a domain at the extreme N terminus of these proteins has been termed the FCH domain, based on homology to Cdc42-interacting protein (CIP4) (5). While the FCH domain in CIP4 confers localization to microtubules (55), the role of this domain in Fps and Fer remains unknown. To delineate the biological function of Fer, a transgenic mouse line was generated in which the *fer* allele was targeted with a kinase-inactivating mutation (fer^{DR}). Surprisingly, $fer^{DR/DR}$ mice are viable and fertile, with no overt defects, but do show defects in platelet-derived growth factor signaling to cortactin (10). A similar kinase-inactivating mutation was engineered into the *fps* locus (fps^{KR}); mice homozygous for this mutation are viable and fertile but display perturbations in cytokine signaling in macrophages (50).

In this study, we used bone marrow-derived mast cells (BMMCs) from $fer^{DR/DR}$ mice to identify the role of Fer in mast cell signaling. We show that the aggregation of FcεRI led to the activation of both Fer and Fps kinases and that Fer was activated downstream of the Kit receptor. Although the phosphorylation of many signaling proteins was unaffected by the loss of Fer, p38 MAP kinase activation was diminished downstream of activated FcεRI and activated Kit receptor. Consistent with the role of p38 kinase in cell migration, Fer-deficient BMMCs displayed reduced motility upon the activation of FcεRI or the Kit receptor. The reintroduction of Fer kinase activity in $fer^{DR/DR}$ cells restored p38 kinase activation and chemotaxis, suggesting that Fer signals to p38 MAP kinase in activated mast cells.

MATERIALS AND METHODS

Mice. Mice bearing a kinase-inactivating mutation (aspartate-743 to arginine) in *fer* (fer^{DR}) were described previously (10). Wild-type and $fer^{DR/DR}$ mice were maintained in an inbred 129×1/SvJ background and housed under specific-pathogen-free conditions at Queen's University Animal Care Services according to Canadian Council on Animal Care regulations.

BMMC cultures. Femurs were isolated asceptically from 4- to 8-week-old wild-type and $fer^{DR/DR}$ mice, and bone marrow cells were isolated by repeated flushing with BMMC medium (Iscove modified Dulbecco medium, 10% [vol/vol] fetal bovine serum, 1% [vol/vol] antimicrobial-antimycotic solution [GibcoBRL], 1 mM sodium pyruvate [GibcoBRL], 1% [vol/vol] nonessential amino acids [GibcoBRL], 1% [vol/vol] conditioned medium from X63-IL-3 cells [32] [kindly provided by Rob Rottapel, University of Toronto], 50 μM α-monothioylglycolate [Sigma]). Cultures were maintained at 0.5×10^6 to 1×10^6/ml of nonadherent cells, with adherent cells being discarded. After >4 weeks of culturing, the purity of BMMCs was monitored by flow cytometry. For the detection of FcεRI, 10^6 BMMCs were incubated overnight with antibody to (α-) dinitrophenyl (DNP)-IgE (1 μg/ml [Sigma] or in some cases 10% [vol/vol] conditioned medium from SPE-7 cells [kindly provided by Juan Rivera, National Institutes of Health]), washed, and then labeled with either α-IgE-fluorescein isothiocyanate (FITC; Southern Biotechnology Associates, Inc.) or isotype control rat IgG1-FITC (BD PharMingen). For the detection of Kit, 10^6 BMMCs were labeled with α-Kit-FITC (BD PharMingen) or isotype control rat IgG2b-FITC (BD PharMingen) and analyzed by flow cytometry.

BMMC stimulation and harvesting. BMMCs were starved overnight in starvation medium (Iscove modified Dulbecco medium, 10% [vol/vol] fetal bovine serum, 1% [vol/vol] antimicrobial-antimycotic solution, 50 μM α-monothioylglycolate) with or without α-DNP-IgE (10% [vol/vol] conditioned medium from SPE-7 cells). Cells were washed in starvation medium, resuspended in prewarmed Tyrodes buffer (10 mM HEPES [pH 7.4], 130 mM NaCl, 5 mM KCl, 1.4 mM $CaCl_2$, 1 mM $MgCl_2$, 5.6 mM glucose, 0.1% bovine serum albumin) with or without DNP-conjugated human serum albumin (HSA; 100 ng/ml; Sigma) or recombinant rat stem cell factor (SCF; R&D Systems), and incubated for various times at 37°C. Cells were then placed on ice, pelleted by centrifugation at 4°C, and washed in phosphate-buffered saline–5 mM EGTA–0.1 mM sodium orthovanadate. Cells were then pelleted and solubilized in kinase lysis buffer (20 mM Tris-HCl [pH 7.5], 150 mM NaCl, 1 mM EDTA, 1% [vol/vol] Nonidet P-40, 0.5% [wt/vol] sodium deoxycholate, 10 μg of aprotinin/ml, 10 μg of leupeptin/ml, 1 mM vanadate, 100 μM phenylmethylsulfonyl fluoride) for 30 min at 4°C on a Nutator. Insoluble material was removed by centrifugation at $12,000 \times g$ to generate soluble cell lysates (SCLs).

Immunoprecipitation and immunoblotting. SCLs (equivalent to 5×10^6 cells/condition) were subjected to immunoprecipitation with the following antibodies: 3 μl of α-FerLA (19) rabbit polyclonal (referred to as α-Fer in this study) and 3 μl of α-FpsQE (19) rabbit polyclonal (referred to as α-Fps/Fer in this study). Antibody-protein complexes were recovered with 20 μl of GammaBind Sepharose (a 50% [vol/vol] slurry in phosphate-buffered saline; Amersham Pharmacia Biotech) and washed three times with 1 ml of kinase lysis buffer. Proteins were recovered by adding 25 μl of 2× sodium dodecyl sulfate sample buffer (130 mM Tris-HCl [pH 6.8], 20% [vol/vol] glycerol, 2% [wt/vol] sodium dodecyl sulfate, 10% [vol/vol] β-mercaptoethanol, 0.08% [wt/vol] bromophenol blue).

Immunoblotting was carried out following the transfer of proteins to Immobilon P membranes (Millipore) by using a semidry transfer apparatus (Bio-Rad). Blots were probed with the following antibodies: α-phosphotyrosine (α-pY) mouse monoclonal (PY99; 1:1,000; Santa Cruz Biotechnology), α-Fer rabbit polyclonal (1:1,000), α-Fps/Fer rabbit polyclonal (1:1,000), α-phosphorylated Erk (α-pErk) mouse monoclonal (1:500; Santa Cruz Biotechnology), α-Erk rabbit polyclonal (1:500; Santa Cruz Biotechnology), α-phosphorylated p38 (α-pp38; Thr180/Tyr182) rabbit polyclonal (1:1,000; Cell Signaling Technology), α-p38 rabbit polyclonal (1:500; Santa Cruz Biotechnology), α-phosphorylated MAP kinase kinase 3 (Mkk3)/Mkk6 (α-pMkk3/6; Ser189/207) rabbit polyclonal (1:1,000; Cell Signaling Technology), and α-Mkk3 rabbit polyclonal (1:1,000; Cell Signaling Technology). Antibody complexes were detected with either horseradish peroxidase-conjugated sheep anti-mouse immunoglobulin (1:5,000; Amersham Pharmacia Biotech) or horseradish peroxidase-conjugated goat anti-rabbit immunoglobulin (1:10,000; Chemicon) and revealed by enhanced chemiluminescence (NEN).

Degranulation. BMMC degranulation was measured by using β-hexoseaminidase as a marker enzyme as described previously (23). Briefly, BMMCs (5×10^5/condition) were starved, sensitized with α-DNP-IgE, and challenged or not challenged with DNP-HSA (100 ng/ml) or the calcium ionophore A23187 (0.5 μM; Sigma) for 30 min at 37°C with agitation. BMMCs were pelleted, and the amounts of β-hexoseaminidase in the supernatant and in the solubilized pellet were measured by using *p*-nitrophenyl *N*-acetyl-β-d-glucosaminidine (Sigma) as a substrate. Percent degranulation was calculated as follows: (released activity/total activity) × 100.

Leukotriene and cytokine secretion. An enzyme-linked immunosorbent assay (ELISA; Amersham Pharmacia Biotech) was used to measure leukotriene levels in cell-free supernatants from BMMCs (10^7) that had been starved overnight in starvation medium with or without α-DNP-IgE (in 10% [vol/vol] conditioned medium from SPE-7 cells) and stimulated with DNP-HSA (100 ng/ml) for 2 h.

The production and release of TNF-α were also measured by an ELISA (BD PharMingen) with the same supernatant samples as those described above.

BMMC adhesion assays. Adhesion assays were performed essentially as previously described (41). Briefly, BMMCs were starved, sensitized with α-DNP-IgE, and labeled with a fluorescent cell-permeating stain (Cell Tracker Green; Molecular Probes). Cells were then stimulated with DNP-HSA (100 ng/ml) or SCF (20 ng/ml) and placed in triplicate fibronectin-coated wells (20 μg/ml) of a 96-well plate (5×10^4 cells/well) for 30 min. Nonadherent cells were removed, wells were washed, and bound fluorescence was measured by fluorimetry (SpectraMax Gemini XS; Molecular Devices).

BMMC chemotaxis assays. Chemotaxis assays were performed essentially as previously described (64). Briefly, BMMCs were starved, sensitized with α-DNP-IgE, and placed in the upper well of a Transwell chamber (8-μm-pore size) containing starvation medium (2.5×10^5 cells/ml). Lower wells contained starvation medium with or without DNP-HSA (100 ng/ml) or SCF (20 ng/ml). Cells were incubated at 37°C for 4 h, and cells that had migrated into the lower wells were counted with a cell counter (Beckman Coulter Counter).

Retroviral transduction of BMMCs. The Fer cDNA bearing a C-terminal Myc epitope-tagged sequence (8, 11) was subcloned into the puromycin-selectable retroviral plasmid pMSCVpac (20). The resulting construct (rescue) and the parental vector (control) were transiently transfected into ϕNX-Eco packaging cells (kindly provided by Garry Nolan, Stanford University). Cells were seeded at 50% confluence in 60-mm plates and transfected with polyethyleneimine (PEI-25; 25,000-Da mean molecular mass; Aldrich) as described previously (65). A cell-free viral supernatant was isolated and filtered (0.2-μm-pore size; Sarsted) 5 days posttransfection and frozen in aliquots at −70°C. $fer^{DR/DR}$ BMMCs (10^7) were resuspended in BMMC medium containing 5 μg of Polybrene/ml (3×10^6/ml) in the presence of control and rescue viruses (1 ml) for 3 days. Cells were recovered, and infections were repeated with fresh medium containing 5 μg of Polybrene/ml and fresh virus for an additional 2 days. Transduced cells were selected in BMMC medium supplemented with puromycin (2 μg/ml) for 7 days. Viable cells were expanded for several weeks in BMMC medium before experimentation.

RESULTS

Activation of both Fer and Fps kinases upon aggregation of FcεRI on BMMCs. It was shown previously with an immortalized mast cell line that along with Lyn and Syk, Fer kinase becomes activated immediately after aggregation of FcεRI by a multivalent antigen (42). Since this initial observation, the role of Fer in mast cell signaling still has not been discovered. Craig et al. recently generated transgenic mice harboring a targeted kinase-inactivating mutation in the *fer* locus (fer^{DR}), and although homozygous mutant mice ($fer^{DR/DR}$) lacked Fer kinase activity and showed reduced Fer protein levels, the mice were viable and fertile, with no overt defects (10). In this study, we generated BMMCs from wild-type and $fer^{DR/DR}$ mice in order to delineate the role of Fer in propagating signals from activated FcεRI. After more than 4 weeks of culturing in the presence of IL-3, the nonadherent BMMCs were highly enriched for mast cells, as shown by the surface expression of FcεRI (Fig. 1A) and high-level expression of the Kit receptor (Fig. 1B). The cytoplasm of cultured cells of both genotypes also exhibited a highly granular appearance in cytospin preparations (Fig. 1C). The numbers of BMMCs obtained were similar for both genotypes, suggesting that Fer is not required for IL-3-dependent proliferation and survival. Also, no differences were observed between wild-type and $fer^{DR/DR}$ BMMCs in apoptosis upon IL-3 withdrawal or survival induced by binding of IgE (data not shown).

To confirm that BMMCs were responsive to FcεRI aggregation, BMMCs were starved and sensitized to DNP via binding of α-DNP-IgE. Cells were then challenged with multivalent DNP-HSA for various times. The overall profiles of tyrosine-phosphorylated proteins were compared for SCLs from wild-type and $fer^{DR/DR}$ BMMCs probed with α-pY antibody (Fig. 2A, upper panel). No differences were observed in basal phosphorylation profiles for starved cells and cells sensitized with IgE antibody (compare lanes 1 and 2 with lanes 6 and 7 in Fig. 2A). Although the amount of phosphorylation appeared

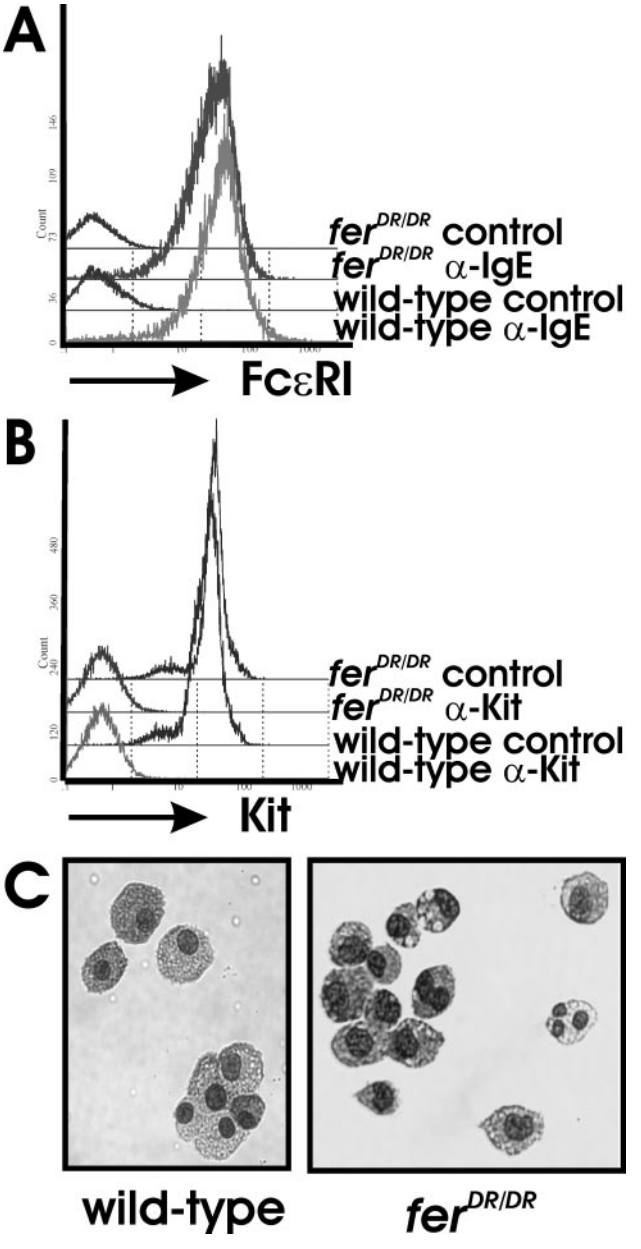

FIG. 1. Maturation of BMMC cultures. Bone marrow cells from wild-type or $fer^{DR/DR}$ mice were grown in the presence of IL-3 and maintained as BMMC cultures as described in Materials and Methods. (A) Surface expression of FcεRI was assessed by flow cytometry by preincubating BMMCs with α-DNP-IgE, followed by staining with FITC-conjugated α-IgE or isotype control antibodies. (B) Surface expression of Kit was analyzed by flow cytometry after staining of BMMCs with FITC-conjugated α-Kit or isotype control antibodies. (C) BMMC morphology was assessed after cytospinning and staining with DiffQuik (Baxter) and was captured by using an RT Color SPOT camera (Diagnostics Instruments Inc.) with an inverted microscope (Leitz Labovert FS; ≈300-fold magnification).

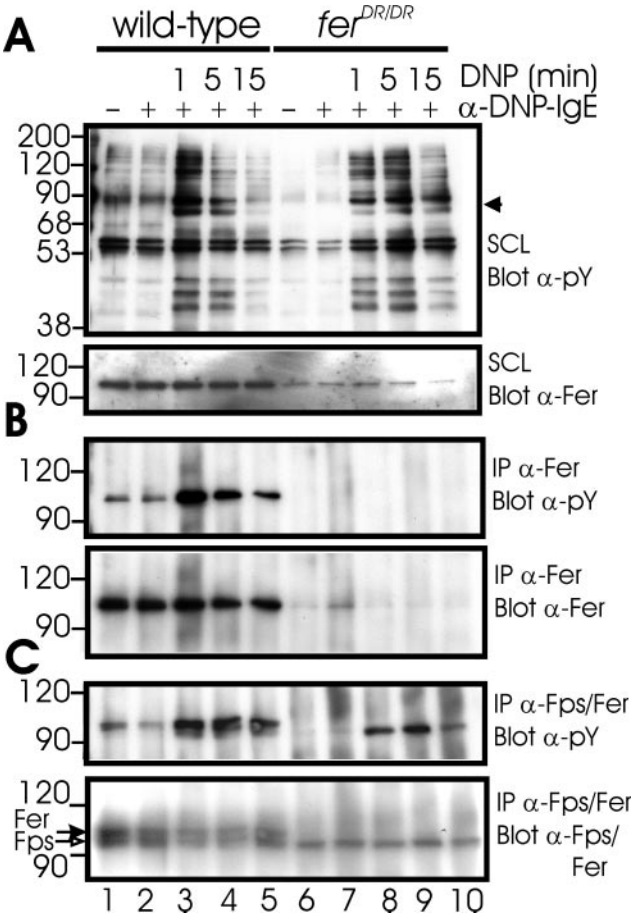

FIG. 2. Increased phosphorylation of Fer and Fps kinases upon aggregation of FcεRI. BMMCs were starved, sensitized with α-DNP-IgE, and challenged or not challenged with DNP-HSA (100 ng/ml) for various times. (A) SCLs were immunoblotted with α-pY and α-Fer antibodies. Proteins displaying reduced phosphorylation in Fer-deficient BMMCs are marked with an arrowhead on the right. (B) Lysates were subjected to immunoprecipitation (IP) with α-Fer serum and immunoblotted with both α-pY and α-Fer antibodies. (C) Lysates were subjected to immunoprecipitation with α-Fps/Fer serum and immunoblotted with both α-pY and α-Fps/Fer antibodies. The positions of p94 Fer and p92 Fps are indicated by arrows on the left. The relative positions of molecular mass markers (in kilodaltons) are indicated on the left.

smaller in $fer^{DR/DR}$ BMMCs (Fig. 2A, lanes 6 and 7), this finding was not consistently observed and likely reflects a slight underloading of the samples. A number of additional phosphoproteins were detected as early as 1 min after aggregation of FcεRI (Fig. 2A, lanes 3 and 8), and while the overall intensities for most of these proteins were slightly lower in $fer^{DR/DR}$ BMMCs, the phosphorylation of an ≈70-kDa protein was dramatically reduced in Fer-deficient BMMCs. Although the identity of this protein is currently unknown, a number of phosphoproteins are possible candidates, including Syk and SLP-76. Fer was readily detected in SCLs from wild-type cells, but its steady-state levels were greatly reduced by the D743R mutation (Fig. 2A, lower panel). The destabilization of FerDR has been observed in a variety of tissues and cell types (10), and there is evidence that this effect is due to ubiquitination and degradation (A. Craig, unpublished data).

To confirm the previous observation of Fer phosphorylation upon FcεRI aggregation (42), lysates were immunoprecipitated with Fer-specific antisera (α-Fer), and phosphorylated Fer was detected with α-pY (Fig. 2B). While some basal phosphorylation of Fer was observed in starved cells (Fig. 2B, lane 1) and in cells treated with IgE alone for 5 min (lane 2), phosphorylation was dramatically elevated upon aggregation of FcεRI for 1 min (lane 3) as well as at later times (lanes 4 and 5). No Fer phosphorylation was observed in $fer^{DR/DR}$ BMMCs (Fig. 2B, lanes 6 to 10). These differences were not due to differences in loading, since reprobing with α-Fer revealed similar amounts of Fer in wild-type cell lysates (Fig. 2B, lanes 1 to 5) and reduced but detectable levels in $fer^{DR/DR}$ cell lysates (lanes 6 to 10). We also performed immunoprecipitation with the same cell lysates and antisera that recognize both Fer and Fps kinases (α-Fps/Fer) (Fig. 2C). For wild-type cell lysates, we observed increased phosphorylation of Fer upon FcεRI aggregation (Fig. 2C, upper panel, lanes 3 to 5). A phosphoprotein migrating slightly faster was also observed upon FcεRI aggregation in wild-type cell lysates (Fig. 2C, lanes 3 to 5); this band was consistent with the size of Fps (92 kDa) but was partially masked by the p94 Fer band. The FcεRI aggregation-induced phosphorylation of Fps was much more readily observed in Fer-deficient cell lysates, where the phosphorylation of Fps was detected at 1, 5, and 15 min poststimulation (Fig. 2C, lanes 8 to 10). Reprobing of the blot with α-Fps/Fer identified a doublet of Fps and Fer in wild-type cell lysates at approximately equimolar amounts (Fig. 2C, lower panel, lanes 1 to 5). In immunoprecipitates from $fer^{DR/DR}$ cell lysates, the amounts of Fer were dramatically reduced, but the levels of Fps were constant (Fig. 2C, lower panel, lanes 6 to 10). These data indicate that in addition to Fer, Fps also becomes highly phosphorylated at between 1 and 5 min after FcεRI aggregation. This is the first description of a common signaling pathway activating Fps and Fer and the first observation of Fps activation by an immunoreceptor signaling pathway.

To determine whether increased phosphorylation of Fer in activated mast cells correlates with increased kinase activity, in vitro kinase assays were performed with Fer immunoprecipitates from starved or FcεRI-stimulated BMMC lysates. We observed increased autophosphorylation of Fer after FcεRI aggregation and elevated phosphorylation of an exogenously added substrate (enolase) in wild-type cell lysates (data not shown). As expected, both autophosphorylation and substrate phosphorylation were decreased in $fer^{DR/DR}$ BMMC lysates. These results are consistent with those of previous studies of Fer and Fps phosphorylation that revealed that the major sites of autophosphorylation reside in the activation loop regions of both kinases (6, 11, 21). Phosphorylation of activation loop residues is a widely used mechanism of kinase activation. Therefore, the tyrosine phosphorylation status of Fer and Fps correlates well with kinase activation.

Phosphorylation of Fer downstream of the activated Kit receptor. In addition to FcεRI signaling, the receptor PTK Kit plays a critical role in mast cell differentiation, proliferation, and function (57, 58). Since Kit displays extensive homology to the platelet-derived growth factor receptor and Fer is activated downstream of the platelet-derived growth factor receptor (10,

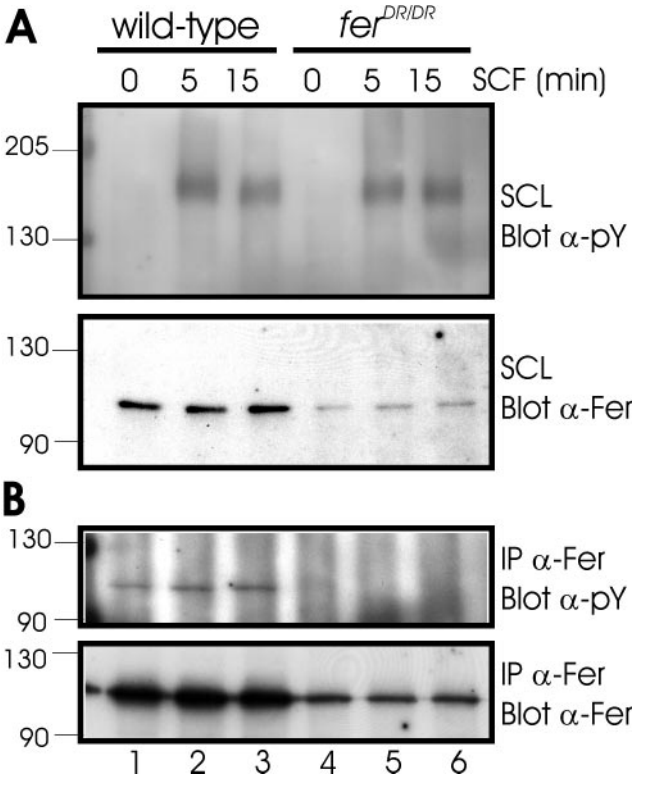

FIG. 3. Increased Fer phosphorylation downstream of the activated Kit receptor. BMMCs were starved and challenged or not challenged with SCF (10 ng/ml) for the indicated times. (A) Lysates were prepared and immunoblotted with α-pY and α-Fer antibodies. (B) Immunoprecipitation was carried out with α-Fer serum, and immunoblotting was done with α-pY and α-Fer antibodies. The positions of molecular mass markers (in kilodaltons) are indicated on the left.

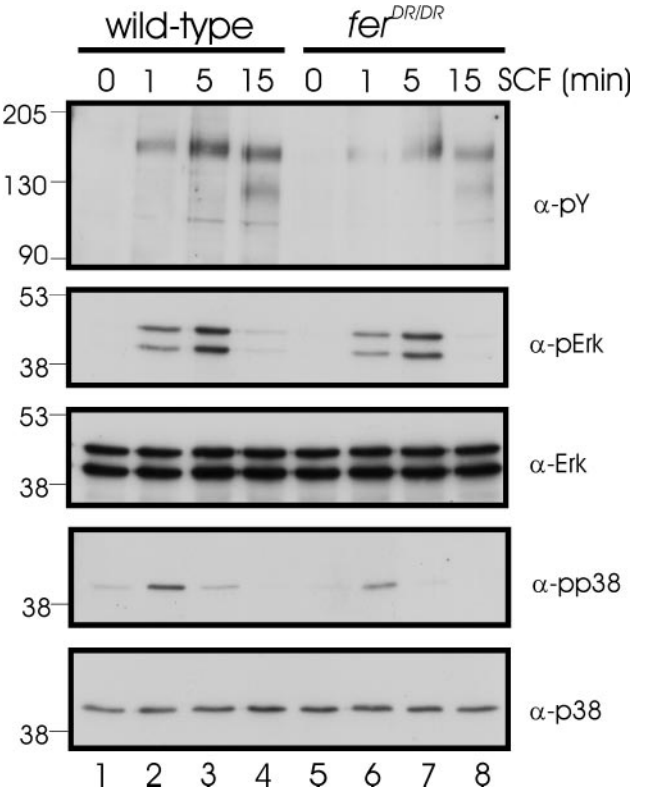

FIG. 4. Fer kinase is required for maximal p38 MAP kinase activation downstream of the activated Kit receptor. BMMCs were starved and challenged or not challenged with SCF (10 ng/ml) for the indicated times. SCLs were immunoblotted with α-pY, α-phosphorylated Erk1/Erk2 (α-pErk), α-Erk1/Erk2 (α-Erk), α-pp38, and α-p38 antibodies. The positions of molecular mass markers (in kilodaltons) are indicated on the left.

33, 34), we analyzed Fer phosphorylation upon Kit activation by SCF treatment of wild-type and *fer*$^{DR/DR}$ BMMCs. Stimulation with SCF for either 5 or 15 min resulted in tyrosine phosphorylation of an ≈150-kDa protein in cells of both genotypes that likely corresponds to Kit (Fig. 3A). Immunoprecipitation of Kit followed by α-pY blotting revealed no differences in overall tyrosine phosphorylation in wild-type and *fer*$^{DR/DR}$ BMMCs (data not shown). Fer phosphorylation was elevated upon SCF stimulation for 5 and 15 min compared to that in starved wild-type cells (Fig. 3B, lanes 1 to 3). No phosphorylation of Fer was evident in *fer*$^{DR/DR}$ cell lysates upon SCF treatment (Fig. 3B, lanes 4 to 6), suggesting an autophosphorylation mechanism for Fer phosphorylation. Despite the reduced steady-state levels of Fer in *fer*$^{DR/DR}$ cell lysates, similar amounts of Fer were recovered in immunoprecipitates from starved and stimulated cell lysates. These results provide the first evidence for Fer activation downstream of the Kit receptor and suggest that Fer plays a role in both FcεRI and Kit signaling in mast cells.

Reduced Kit signaling to p38 MAP kinase in *fer*$^{DR/DR}$ BMMCs. In order to identify signaling pathways downstream of Kit that Fer may regulate, we assessed the activation of the MAP kinases. Wild-type and *fer*$^{DR/DR}$ BMMCs were starved and treated with SCF for various times (Fig. 4). SCLs immunoblotted with α-pY revealed similar profiles of tyrosine phosphorylation between the genotypes. Analysis of Erk MAP kinase phosphorylation revealed peak phosphorylation at 5 min after Kit activation and no differences between wild-type and *fer*$^{DR/DR}$ cells (compare lanes 3 and 7 in Fig. 4). Blotting with a control Erk1/Erk2 antibody revealed similar levels of loading between samples. Characterization of p38 MAP kinase phosphorylation revealed peak phosphorylation after SCF treatment for 1 min, but the amount of p38 phosphorylation was greatly reduced in *fer*$^{DR/DR}$ cell lysates (compare lanes 2 and 6 in Fig. 4). The reduced phosphorylation was not due to differences in loading or expression levels, as similar amounts of p38 were detected in all samples. These results suggest that Fer kinase is involved in mediating p38 MAP kinase activation downstream of Kit.

Role of Fer in FcεRI signaling to p38 MAP kinase. To explore the role of Fer in FcεRI signaling, we compared FcεRI aggregation-induced phosphorylation in wild-type and *fer*$^{DR/DR}$ BMMCs for a number of proteins known to play roles in mast cell signaling. FcεRI aggregation-induced phosphorylation of Lyn, Syk, linker of activated T cells (LAT), Btk, phospholipase C-γ, Vav, and Src homology 2-containing inositol phosphatase 1 was unaffected by the loss of Fer kinase activity (data not shown). We did, however, observe reduced phosphorylation of cortactin in *fer*$^{DR/DR}$ BMMCs (data not shown), but the level of expression of cortactin was much lower than that observed in

other cell systems, where cortactin is known to regulate the actin cytoskeleton. HS1 is highly homologous to cortactin and becomes tyrosine phosphorylated upon FcεRI aggregation in mast cells (16). It will be interesting to determine whether HS1 is a substrate of Fer in mast cells.

To address whether activation of the major downstream signaling pathways occurs normally in the absence of Fer, a time course experiment was performed to assess the phosphorylation of the MAP kinases after FcεRI aggregation. The overall profiles of tyrosine phosphorylation in SCLs were also assessed after immunoblotting with α-pY, which revealed increased phosphorylation of a number of proteins at 1 and 2 min after FcεRI aggregation (Fig. 5, lanes 2, 3, 6, and 7). The profiles of tyrosine phosphorylation were comparable for lysates of cells of both genotypes, with the exception of an ≈70-kDa protein that displayed reduced phosphorylation in Fer-deficient BMMCs. Overall phosphorylation was greatly reduced by 25 min poststimulation in cells of both genotypes. Phosphorylation of Erk1 and Erk2 MAP kinases was observed at 1 min (Fig. 5, lanes 2 and 6) and at 5 min (lanes 3 and 7) but was diminished by 25 min after FcεRI aggregation, with no differences being observed between genotypes (lanes 4 and 8). Blotting with a control antibody showed equal levels of loading for wild-type and *fer*$^{DR/DR}$ cell lysates (Fig. 5, third panel from top, lanes 1 to 8). Therefore, Fer kinase activation is not required for Erk activation.

We also examined the phosphorylation of p38 MAP kinase, which was detected at 1 and 5 min (Fig. 5, lanes 2, 3, 6, and 7) but not at 25 min (lanes 4 and 8) after receptor activation. However, the kinetics of p38 activation were different for the wild-type and *fer*$^{DR/DR}$ BMMCs, with maximal activation being observed at 5 min poststimulation for wild-type cells compared to reduced phosphorylation of p38 at 5 min poststimulation for *fer*$^{DR/DR}$ cells (compare lanes 3 and 7 in Fig. 5). Blotting with a control p38 antibody revealed similar levels of loading between samples. The reduced p38 phosphorylation in Fer-deficient cells was reproducibly observed with independently generated BMMC cultures (data not shown). These results were consistent with those shown above (Fig. 4) and suggested that Fer kinase is required in mast cells for maximal p38 activation downstream of both FcεRI and the Kit receptor.

To determine whether Fer kinase acts upstream of p38 in the signaling pathway (15), the phosphorylation of Mkk3 and Mkk6 was assessed. In wild-type cells, the phosphorylation of Mkk3 and Mkk6 was elevated at both 1 and 5 min poststimulation (Fig. 5, lanes 2 and 3). However, in *fer*$^{DR/DR}$ cells, the activation of Mkk3 and Mkk6 was greatly diminished and was not as sustained as in wild-type cells (compare lanes 6 and 7 with lanes 2 and 3 in Fig. 5). The overall amounts of Mkk3 in *fer*$^{DR/DR}$ cell lysates were slightly reduced (Fig. 5, lanes 5 to 8), but some of the apparent loading differences reflect incomplete stripping of α-pMkk3/6 antibody. These observations suggest that Fer kinase acts upstream of Mkk3 and Mkk6 in p38 MAP kinase activation.

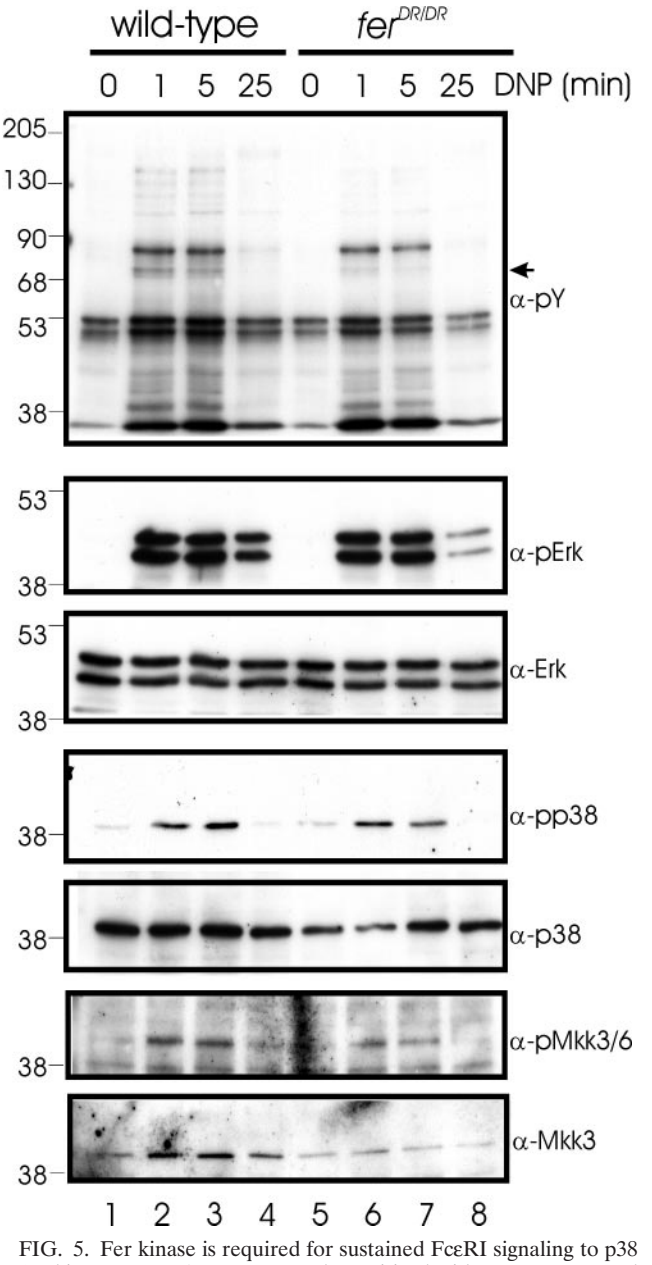

FIG. 5. Fer kinase is required for sustained FcεRI signaling to p38 MAP kinase. BMMCs were starved, sensitized with α-DNP-IgE, and challenged or not challenged with DNP-HSA (100 ng/ml) for the indicated times. SCLs were prepared and subjected to immunoblotting with α-pY, α-pErk, α-pp38, and α-pMkk3/6 antibodies as well as control antibodies to Erk, p38, and Mkk3. The position of a 70-kDa protein that is hypophosphorylated in *fer*$^{DR/DR}$ cells is indicated by an arrow on the right. The positions of molecular mass markers (in kilodaltons) are indicated on the left.

Normal secretion responses in activated Fer-deficient BMMCs. To examine some of the physiological responses of Fer-deficient mast cells, we measured degranulation, leukotriene production, and cytokine secretion (Fig. 6). FcεRI aggregation leads to the release of calcium from intracellular stores, which triggers degranulation. We assayed degranulation by measuring β-hexoseaminidase activity released from cells with a colorimetric assay. Low-level degranulation was observed in starved and sensitized BMMCs, with no differences between wild-type and *fer*$^{DR/DR}$ cells (Fig. 6A). Aggregation of FcεRI with DNP-HSA led to increased degranulation in both wild-type and *fer*$^{DR/DR}$ BMMCs. More substantial degranulation was observed when cells were treated with the calcium iono-

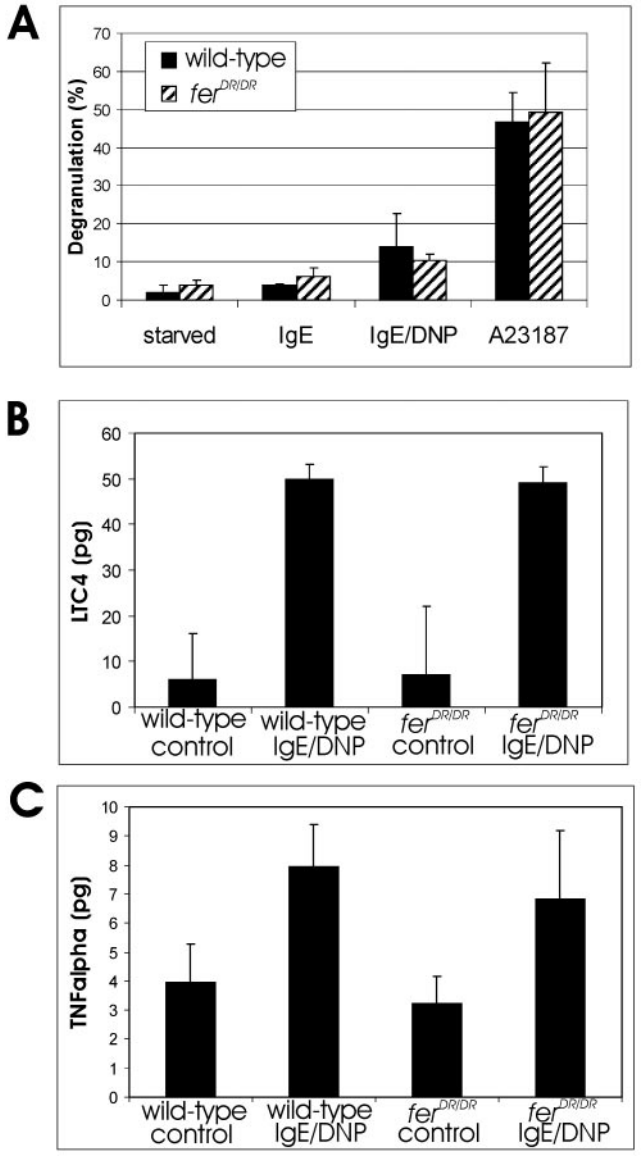

FIG. 6. Fer kinase is not required for degranulation and secretion of leukotrienes and cytokines. (A) BMMCs (5×10^5/condition) were starved, sensitized with α-DNP-IgE, and challenged or not challenged with DNP-HSA (100 ng/ml) or with the calcium ionophore A23187 (0.5 μM) for 30 min. BMMCs were pelleted, and the amounts of β-hexosaminidase in the supernatant and in the solubilized pellet were measured. Percent degranulation was calculcated as (released activity/total activity) × 100 for three separate experiments with samples measured in triplicate. Error bars indicate standard deviations. (B) An ELISA was used to measure LTC_4 levels in cell-free supernatants from BMMCs (10^7) that were starved, sensitized with α-DNP-IgE, and stimulated with DNP-HSA (100 ng/ml) for 2 h. Values given are means and standard deviations for three separate experiments. (C) An ELISA was used to measure the secretion of TNF-α in cell-free supernatants from BMMCs (10^7) that were starved, sensitized with α-DNP-IgE, and stimulated with DNP-HSA (100 ng/ml) for 2 h. Values given are means and standard deviations for three separate experiments.

phore A23187, which causes a rapid influx of calcium. However, no differences were observed between genotypes.

Activated mast cells also synthesize and secrete leukotrienes, and we measured leukotriene levels in cell-free supernatants from starved or FcεRI-activated BMMCs. Leukotrienes were detected at appreciable levels only after FcεRI aggregation, with similar levels being observed for BMMCs of both genotypes (Fig. 6B). Therefore, signaling to lipid mediator production does not require Fer kinase activity.

Mast cells also synthesize and secrete a vast array of cytokines upon FcεRI aggregation. At the level of transcription, we observed no defects in the upregulation of IL-4, IL-5, IL-13, or gamma interferon in Fer-deficient BMMCs (data not shown). We also measured the production and secretion of TNF-α in cell-free supernatants from stimulated BMMCs (Fig. 6C). As is the case for leukotriene production, no differences were observed in TNF-α secretion from wild-type and $fer^{DR/DR}$ BMMCs. Therefore, Fer is not required for signaling to the nucleus to upregulate cytokine gene expression.

Increased adhesion and reduced motility in Fer-deficient BMMCs. In addition to changes in gene expression and secretion of inflammatory mediators, mast cell activation downstream of either FcεRI or the Kit receptor leads to increased cell adhesion (13, 53). To determine whether Fer kinase is required for changes in cell adhesion after mast cell stimulation, we compared the abilities of wild-type and $fer^{DR/DR}$ BMMCs to adhere to fibronectin-coated wells (Fig. 7A). Under starvation conditions, very low levels of cell adhesion were detected for wild-type cells, whereas Fer-deficient BMMCs displayed slightly elevated adhesion. When mast cells were treated with SCF to activate Kit, increased adhesion of both wild-type and $fer^{DR/DR}$ BMMCs was evident. Mast cells were also sensitized to DNP by pretreatment with α-DNP-IgE (Fig. 7A, IgE baseline), without a change in their adhesion properties (compared to starvation conditions). Upon stimulation of FcεRI with DNP-HSA treatment, both wild-type and $fer^{DR/DR}$ BMMCs showed elevated adhesion (compared to the IgE baseline). These data show that Fer-deficient BMMCs are slightly more adherent than wild-type BMMCs under both starvation and stimulation conditions. These data are consistent with the results of previous studies that implicated Fer in regulating cell adhesion in other cell systems (3, 37, 38, 47).

Mast cells also display increased motility upon activation of FcεRI and Kit signaling (27, 54, 64). Since we observed reduced p38 activation in $fer^{DR/DR}$ BMMCs (Fig. 4 and 5), we postulated that differences in motility might also be observed. We measured motility by counting the numbers of starved or α-DNP-IgE-sensitized BMMCs that migrated through pores toward a concentration gradient of SCF or DNP-HSA (Fig. 7B). Under starvation conditions, few wild-type and $fer^{DR/DR}$ BMMCs migrated to the lower wells. However, in the presence of SCF, wild-type BMMCs showed dramatically elevated motility, whereas Fer-deficient BMMCs responded only marginally to the chemotactic factor. Likewise, when DNP-sensitized mast cells (Fig. 7B, IgE) were cultured in the presence of DNP-HSA in the lower wells, wild-type BMMCs displayed increased motility (Fig. 7B, IgE/DNP). In contrast, $fer^{DR/DR}$ BMMCs showed only a small increase in motility upon FcεRI aggregation. These results suggest that Fer kinase is required for FcεRI and Kit signaling to p38 MAP kinase to promote the chemotaxis of activated mast cells.

Rescue of p38 MAP kinase signaling and chemotaxis by expression of active Fer kinase in $fer^{DR/DR}$ BMMCs. To lend further support to our results suggesting a role for Fer kinase

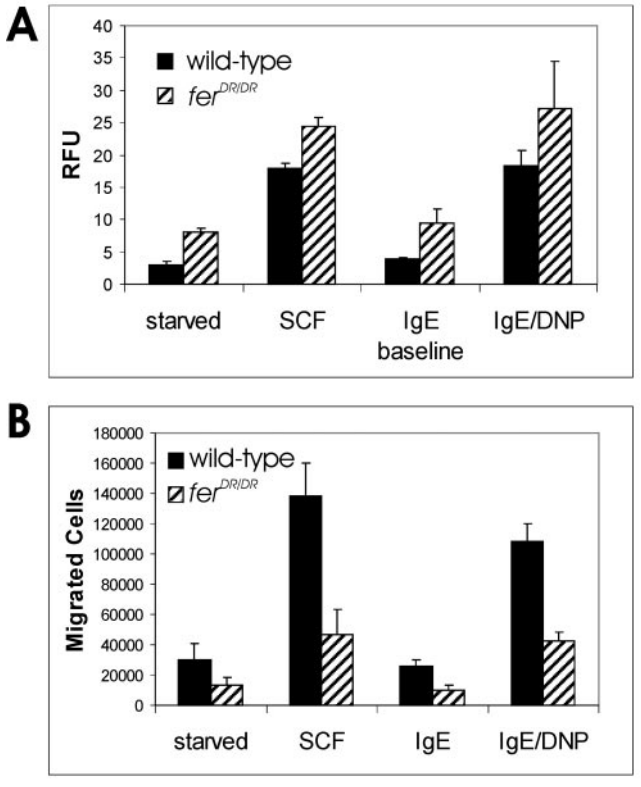

FIG. 7. Elevated cell adhesion and reduced chemotaxis in Fer-deficient BMMCs. (A) BMMCs were starved, sensitized with α-DNP-IgE, and labeled with a fluorescent cell-permeating stain (Cell Tracker Green). Cells were then stimulated with DNP-HSA (100 ng/ml) or SCF (20 ng/ml) and placed in triplicate fibronectin-coated wells of a 96-well plate for 30 min. Nonadherent cells were removed, wells were washed, and bound fluorescence was measured by fluorimetry. Values given are relative fluorescence units (RFU) and standard errors of the mean for triplicate samples. (B) BMMCs were starved, sensitized with α-DNP-IgE, and placed in the upper well of a Transwell chamber (8-μm-pore size). Lower wells contained medium with or without DNP-HSA (100 ng/ml) or SCF (20 ng/ml). Cells were incubated at 37°C for 4 h, and cells that migrated were counted by using a Coulter Counter. Values given are means and standard deviations for triplicate samples.

in p38 MAP kinase signaling, we attempted to rescue $fer^{DR/DR}$ BMMCs by retroviral transduction with a control virus or a Myc epitope-tagged Fer kinase-expressing virus (Fig. 8A). The overall profiles of tyrosine phosphorylation were compared for control virus-infected cells (control) and Myc-Fer virus-infected cells (rescue) following FcεRI aggregation (Fig. 8B). Both control and rescue cells responded maximally at 2 min poststimulation, but several phosphoproteins were overrepresented in the rescue cells, including an ≈70-kDa phosphoprotein. Interestingly, we noted previously a reduction in the phosphorylation of a similarly sized protein in $fer^{DR/DR}$ cells compared to wild-type cells (Fig. 2 and 5). The identification of this protein along with several higher-molecular-weight proteins (Fig. 8B) could provide further insight into the role of Fer kinase in mast cell signaling. The expression of Myc-Fer was confirmed by immunoblotting with α-Fer, which detected only FerDR in control cells and an additional protein whose size of 120 kDa corresponds to the size of Myc-Fer. Catalytically active Myc-Fer was expressed at much higher levels than FerDR, but its expression was similar to Fer expression in wild-type cells (data not shown). We next analyzed p38 activation in control and rescue cells. This analysis revealed comparable levels of p38 phosphorylation at 2 min but dramatically elevated phosphorylation at 10 min poststimulation in the rescue cells. These differences were not due to loading, as shown in the immunoblot with a control p38 antibody. Further analysis of the upstream p38-activating kinases Mkk3 and Mkk6 revealed elevated phosphorylation in rescue cells compared to control cells. These results lend further support to a role for Fer kinase in promoting sustained p38 activation.

The motilities of sensitized control and rescue cells toward antigen were also compared (Fig. 8C). Control cells showed only marginal motility toward antigen (Fig. 8C, IgE/DNP), whereas rescue cells displayed a chemotactic response similar to that observed for wild-type cells (Fig. 7B). These data are consistent with the requirement of p38 MAP kinase activation for the chemotaxis of mast cells (27) and implicate Fer kinase as an amplifier of signaling to p38 MAP kinase (Fig. 9).

DISCUSSION

In this report, we describe the activation of PTK Fer upon FcεRI aggregation on BMMCs, consistent with a previous report in which an immortalized mast cell line was used (42). In addition, we show that the highly related PTK Fps is also activated after engagement of FcεRI. This report represents the first description of a common signaling pathway that activates Fer and Fps and also is the first description of Fps activation downstream of an ITAM. Recently, we also observed the activation of both Fer and Fps upon collagen-induced signaling in platelets via ITAM-containing GPVI (Y. Senis and P. Greer, submitted for publication). GPVI shares the γ chain from FcεRI, suggesting that Fer and Fps activation may occur downstream of the recruitment of Syk to ITAMs on the γ chain of the receptor. Currently, we do not fully understand the mechanism of activation, and it will be interesting to determine whether Fer and Fps interact directly with activated receptors or whether other early-acting kinases, such as Lyn (and the Lyn-related kinase Fyn in platelets) or Syk, phosphorylate and activate these kinases. There is evidence from fibroblasts for a role of Fyn in Fer activation upon changes in cell volume (31). Whether a similar dependence on Src family kinases (SFK) exists for Fer activation in mast cells warrants further investigation. The action of an upstream kinase is plausible for the activation of Fps in mast cells, since tyrosine phosphorylation of kinase-dead Fps in FcεRI-stimulated $fps^{KR/KR}$ BMMCs has been observed (Craig, unpublished data). We are currently extending our analysis to signaling in $fps^{KR/KR}$ BMMCs to identify substrates of Fps and to determine the pathways in which it acts. Compound mutant mice lacking both Fer and Fps kinase activities ($fps^{KR/KR}$ $fer^{DR/DR}$) were also recently generated (Y. Senis, A. Craig, and P. Greer, submitted for publication). BMMCs derived from these mice will be used to identify potential common substrates whose phosphorylation may not be affected by inactivation of only Fer or Fps. Using this full complement of genotypes, we hope to fully delineate the roles of Fer and Fps in mast cell signaling.

In this study, we focused on the role of Fer in mast cell

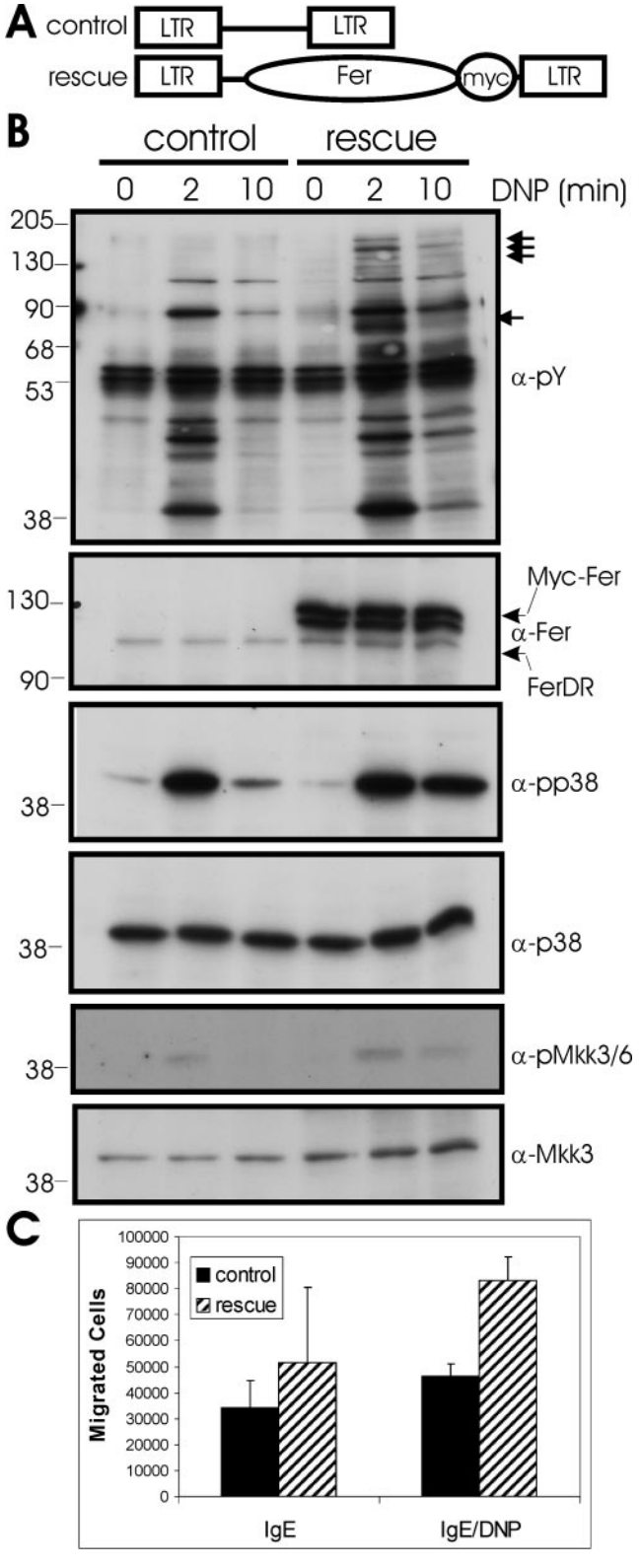

FIG. 8. Rescue of p38 MAP kinase activation and chemotaxis of $fer^{DR/DR}$ BMMCs. (A) Schematic representation of the parental retroviral vector (control) and a retroviral construct designed to express a catalytically active Myc-epitope-tagged Fer kinase (rescue). LTR, long terminal repeat. (B) $fer^{DR/DR}$ BMMCs were infected with control and rescue viruses, and selection was performed with puromycin as described in Materials and Methods. BMMCs were sensitized with α-DNP-IgE and stimulated with DNP-HSA (100 ng/ml) for the indicated times. SCLs were immunoblotted with α-pY, α-Fer, α-pp38, α-p38, α-pMkk3/6, and α-Mkk3 antibodies. The positions of several hyperphosphorylated proteins in the rescue cells are indicated by arrows on the right. The positions of molecular mass markers (in kilodaltons) are indicated on the left. (C) The migration of DNP-sensitized control and rescue BMMCs was measured in the absence and presence of DNP-HSA (100 ng/ml) in the lower wells of a Transwell chamber. Mean values for cells present in the lower wells after 4 h of incubation at 37°C were plotted for quadriplicate samples. Error bars indicate standard deviations.

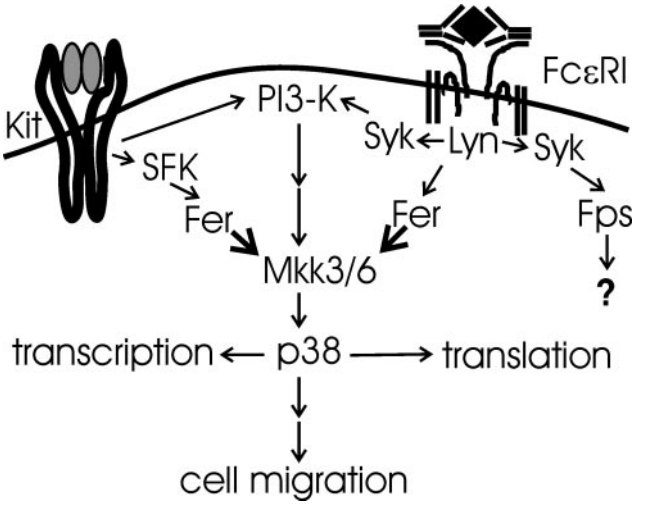

FIG. 9. Model for Fer and Fps kinase signaling in mast cells. Dimeric FcεRI is depicted with bound IgE and antigen, which triggers Lyn activation and the recruitment and activation of Syk. These events may precede Fer and Fps activation. Targets of Fps in mast cells remain unknown. Fer plays an amplifying role in FcεRI-induced p38 MAP kinase activation and chemotaxis, likely acting upstream of Mkk3 and Mkk6. Binding of dimeric SCF to the Kit receptor results in dimerization and activation by transphosphorylation, leading to recruitment and activation of PI3-K and Src family kinase (SFK). SFK and PI3-K activation plays a role in Kit signaling to p38 and chemotaxis. Fer activation may occur downstream of SFK, based on previous results obtained with other cell types. In addition to promoting chemotaxis, p38 MAP kinase regulates transcription and mRNA translation.

signaling by using a transgenic mouse line ($fer^{DR/DR}$) that expresses kinase-inactive Fer (10). In addition to confirming that Fer is activated downstream of FcεRI, we show that the treatment of BMMCs with SCF, which activates the Kit receptor, leads to increased Fer phosphorylation. This is a novel observation that suggests a role for Fer in FcεRI and Kit signaling pathways. The main signaling defect observed in Fer-deficient mast cells involved the activation of p38 MAP kinase. The phosphorylation of p38 was not abolished in $fer^{DR/DR}$ BMMCs; rather, it was less sustained than that in wild-type BMMCs. Consistent with the established role of p38 MAP kinase in cell migration downstream of FcεRI and the Kit receptor (27, 59), $fer^{DR/DR}$ BMMCs displayed impaired migration toward SCF or antigen. Interestingly, retroviral transduction of $fer^{DR/DR}$ BMMCs with a Fer-expressing virus restored sustained p38 activation and chemotactic responses. Therefore, a working model

has been proposed to place our findings in context with previous studies (Fig. 9).

Ishizuka and coworkers described two major pathways involved in mast cell chemotaxis, namely, the p38 MAP kinase pathway and the Rho/Rho-associated coiled-coil-forming protein kinase pathway (26). The activation of phosphatidylinositol 3-kinase (PI3-K) is required for p38 activation downstream of FcεRI but not the Kit receptor (26). However, PI3-K is activated downstream of the Kit receptor and plays a role in chemotaxis (59). Our data suggest a role for Fer in a parallel pathway that acts upstream of the p38-activating kinases Mkk3 and Mkk6. However, this effect is likely not a direct effect of Fer on Mkk3 and Mkk6, since these kinases are activated by serine/threonine phosphorylation within subdomain VIII by MAP kinase kinase kinases (63). Candidate MAP kinase kinase kinases that activate Mkk3 and Mkk6 include TAK1 (51), ASK1 (25), p21-activated kinase (PAK) (36), and MLK-3 (56). The activation of PAK has been shown to involve the binding of PAK-interacting exchange factor, which contains a pleckstrin homology domain and is therefore recruited to the plasma membrane upon PI3-K activation. PAK-interacting exchange factor activates Cdc42/Rac and PAK in a signaling pathway that leads to p38 activation and cytoskeletal rearrangements in fibroblasts (36). It will be interesting to determine whether this pathway is used in mast cells to promote chemotaxis upon FcεRI and Kit receptor activation.

Fer and Fps possess an N-terminal motif termed the FCH domain, which was first described for CIP4 (5). This domain in CIP4 binds microtubules and has been shown to release Wiskott-Aldrich syndrome protein from the actin cytoskeleton and to relocalize Wiskott-Aldrich syndrome protein to microtubules (55). A growing number of FCH domain-containing proteins have been identified, and the vast majority of these proteins associate with the cytoskeleton (reviewed in reference 18). It will be important to determine the role of the FCH domains of Fer and Fps and whether they also confer an association with microtubules or other cytoskeletal networks.

While no major differences in the FcεRI aggregation-induced tyrosine phosphorylation profiles were observed in Fer-deficient BMMCs, we noted reduced phosphorylation of an ≈70-kDa protein. Interestingly, hyperphosphorylation of a similarly sized protein along with several higher-molecular-weight proteins was observed in $fer^{DR/DR}$ cells rescued via the expression of Myc-Fer. These cell lines will be used to try to identify downstream substrates of Fer in mast cells. An obvious candidate phosphoprotein close to 70 kDa in size is Syk, but direct characterization of Syk phosphorylation, as well as other downstream substrates, revealed no obvious defect in Syk activation (data not shown). Another phosphoprotein of a similar size that plays a role in FcεRI signaling is SLP-76. However, the ≈70-kDa protein that is underphosphorylated in $fer^{DR/DR}$ cells is likely not SLP-76, since it is required for degranulation and cytokine production (43), both of which are unaffected by the loss of Fer. Another possible candidate is HS1 (also called SPY-75), which is phosphorylated upon FcεRI aggregation (16) and exhibits a high degree of homology to cortactin (35, 49). Future studies will be required to identify additional Fer substrates in mast cells.

Fer has also been implicated in regulating cadherin- and integrin-mediated cell adhesion in a variety of cell types, including retinal neurites (3, 37, 38) and Fer-overexpressing fibroblasts (47). The current model based on these studies and others is that Fer activation leads to the disruption of cell adhesion, either by phosphorylating the catenins that bridge cadherins to the actin cytoskeleton or by disrupting focal adhesions that are critical for integrin-mediated adhesion. While the precise mechanism of cell adhesion regulation by Fer is currently unknown, overexpression of Fer causes reduced cell adhesion (47). In this study, we show that Fer-deficient BMMCs display increased adhesion to fibronectin when activated either by SCF or through FcεRI clustering. These findings are consistent with the model proposing that Fer activation leads to reduced cell adhesion.

The results of this study suggest that Fer may be important for the recruitment of mast cells to sites of inflammation in vivo. McCafferty et al. performed inflammatory challenges of $fer^{DR/DR}$ mice, including active antigen-dependent hypersensitivity reactions, and found no defects in vessel permeabilization (39). These results are consistent with normal degranulation and leukotriene production by Fer-deficient mast cells. In the same study, increased leukocyte adhesion and emigration upon lipopolysaccharide (LPS)-induced inflammation in $fer^{DR/DR}$ mice were also observed. These results suggest that Fer may play a role in limiting innate immune responses through effects on cell adhesion and emigration. Interestingly, the upregulation of endothelial cell adhesion molecules by LPS and TNF-α occurs in part via p38 MAP kinase activation (29). The p38 MAP kinase pathway has also been implicated in the inhibition of signaling by anti-inflammatory cytokines, such as IL-10 (2). Given the role of Fer in p38 MAP kinase activation in mast cells, it will be important to determine whether p38 MAP kinase activation by LPS or TNF-α is affected in $fer^{DR/DR}$ mice.

In conclusion, FcεRI clustering leads to the activation of both Fer and Fps kinases, representing the first common signaling pathway so far described. However, in Fer-deficient BMMCs, Fps does not compensate for the loss of Fer in signaling to p38 MAP kinase downstream of FcεRI or the Kit receptor to promote mast cell migration. Further experiments are needed to identify the substrates of Fps in FcεRI signaling. The Fer- and Fps-deficient mouse lines that we have generated should prove invaluable in delineating the roles of these highly related PTKs in mast cell function in vivo.

ACKNOWLEDGMENTS

We thank Derek Schulze, Karen Williams, Michelle Scott, and Shuhong Cao for excellent technical assistance. We also gratefully acknowledge Gerald Krystal, Garry Nolan, Robert Hawley, Rob Rottapel, and Juan Rivera for providing reagents and Jacqueline Damen and Gerald Krystal for providing protocols and advice on mast cell cultures. We also thank Yotis Senis for helpful comments on the manuscript.

A.W.B.C is supported by a senior research fellowship from the Canadian Institutes for Health Research (CIHR). This work was supported by grants to P.A.G. from CIHR and the National Cancer Institute of Canada with funds from the Canadian Cancer Society.

REFERENCES

1. **Abraham, S. N., and R. Malaviya.** 1997. Mast cells in infection and immunity. Infect. Immun. **65:**3501–3508.
2. **Ahmed, S. T., and L. B. Ivashkiv.** 2000. Inhibition of IL-6 and IL-10 signaling and Stat activation by inflammatory and stress pathways. J. Immunol. **165:** 5227–5237.

3. **Arregui, C., P. Pathre, J. Lilien, and J. Balsamo.** 2000. The nonreceptor tyrosine kinase fer mediates cross-talk between N-cadherin and beta1-integrins. J. Cell Biol. **149:**1263–1274.
4. **Asai, K., J. Kitaura, Y. Kawakami, N. Yamagata, M. Tsai, D. P. Carbone, F. T. Liu, S. J. Galli, and T. Kawakami.** 2001. Regulation of mast cell survival by IgE. Immunity **14:**791–800.
5. **Aspenstrom, P.** 1997. A Cdc42 target protein with homology to the non-kinase domain of FER has a potential role in regulating the actin cytoskeleton. Curr. Biol. **7:**479–487.
6. **Ben-Dor, I., O. Bern, T. Tennenbaum, and U. Nir.** 1999. Cell cycle-dependent nuclear accumulation of the p94fer tyrosine kinase is regulated by its NH2 terminus and is affected by kinase domain integrity and ATP binding. Cell Growth Differ. **10:**113–129.
7. **Cheng, H. Y., A. P. Schiavone, and T. E. Smithgall.** 2001. A point mutation in the N-terminal coiled-coil domain releases c-Fes tyrosine kinase activity and survival signaling in myeloid leukemia cells. Mol. Cell. Biol. **21:**6170–6180.
8. **Cole, L. A., R. Zirngibl, A. W. Craig, Z. Jia, and P. Greer.** 1999. Mutation of a highly conserved aspartate residue in subdomain IX abolishes Fer protein-tyrosine kinase activity. Protein Eng. **12:**155–162.
9. **Costello, P. S., M. Turner, A. E. Walters, C. N. Cunningham, P. H. Bauer, J. Downward, and V. L. Tybulewicz.** 1996. Critical role for the tyrosine kinase Syk in signalling through the high affinity IgE receptor of mast cells. Oncogene **13:**2595–2605.
10. **Craig, A. W., R. Zirngibl, K. Williams, L. A. Cole, and P. A. Greer.** 2001. Mice devoid of Fer protein-tyrosine kinase activity are viable and fertile but display reduced cortactin phosphorylation. Mol. Cell. Biol. **21:**603–613.
11. **Craig, A. W. B., R. Zirngibl, and P. Greer.** 1999. Disruption of coiled-coil domains in Fer protein-tyrosine kinase abolishes trimerization but not kinase activation. J. Biol. Chem. **274:**19934–19942.
12. **Daeron, M.** 1997. Fc receptor biology. Annu. Rev. Immunol. **15:**203–234.
13. **Dastych, J., and D. D. Metcalfe.** 1994. Stem cell factor induces mast cell adhesion to fibronectin. J. Immunol. **152:**213–219.
14. **Dogar, J. H., G. G. Nemeth, J. M. Durdik, and S. C. Dreskin.** 1993. Fc epsilon RI-mediated expression of mRNA for c-fos in rat basophilic leukemia cells does not require ongoing aggregation of the receptor. Cell. Signal. **5:**605–613.
15. **Enslen, H., J. Raingeaud, and R. J. Davis.** 1998. Selective activation of p38 mitogen-activated protein (MAP) kinase isoforms by the MAP kinase kinases MKK3 and MKK6. J. Biol. Chem. **273:**1741–1748.
16. **Fukamachi, H., N. Yamada, T. Miura, T. Kato, M. Ishikawa, E. Gulbins, A. Altman, Y. Kawakami, and T. Kawakami.** 1994. Identification of a protein, SPY75, with repetitive helix-turn-helix motifs and an SH3 domain as a major substrate for protein tyrosine kinase(s) activated by Fc epsilon RI cross-linking. J. Immunol. **152:**642–652.
17. **Galli, S. J., and B. K. Wershil.** 1996. The two faces of the mast cell. Nature **381:**21–22.
18. **Greer, P.** 2002. Closing in on the biological functions of fps/fes and fer. Nat. Rev. Mol. Cell. Biol. **3:**278–289.
19. **Haigh, J., J. McVeigh, and P. Greer.** 1996. The fps/fes tyrosine kinase is expressed in myeloid, vascular endothelial, epithelial, and neuronal cells and is localized in the trans-Golgi network. Cell Growth Differ. **7:**931–944.
20. **Hawley, R. G., F. H. Lieu, A. Z. Fong, and T. S. Hawley.** 1994. Versatile retroviral vectors for potential use in gene therapy. Gene Ther. **1:**136–138.
21. **Hjermstad, S. J., K. L. Peters, S. D. Briggs, R. I. Glazer, and T. E. Smithgall.** 1993. Regulation of the human c-fes protein tyrosine kinase (p93c-fes) by its src homology 2 domain and major autophosphorylation site (Tyr-713). Oncogene **8:**2283–2292.
22. **Holowka, D., and B. Baird.** 2001. Fc(epsilon)RI as a paradigm for a lipid raft-dependent receptor in hematopoietic cells. Semin. Immunol. **13:**99–105.
23. **Huber, M., C. D. Helgason, J. E. Damen, L. Liu, R. K. Humphries, and G. Krystal.** 1998. The Src homology 2-containing inositol phosphatase (SHIP) is the gatekeeper of mast cell degranulation. Proc. Natl. Acad. Sci. USA **95:**11330–11335.
24. **Hutchinson, L. E., and M. A. McCloskey.** 1995. Fc epsilon RI-mediated induction of nuclear factor of activated T-cells. J. Biol. Chem. **270:**16333–16338.
25. **Ichijo, H., E. Nishida, K. Irie, P. ten Dijke, M. Saitoh, T. Moriguchi, M. Takagi, K. Matsumoto, K. Miyazono, and Y. Gotoh.** 1997. Induction of apoptosis by ASK1, a mammalian MAPKKK that activates SAPK/JNK and p38 signaling pathways. Science **275:**90–94.
26. **Ishizuka, T., K. Chayama, K. Takeda, E. Hamelmann, N. Terada, G. M. Keller, G. L. Johnson, and E. W. Gelfand.** 1999. Mitogen-activated protein kinase activation through Fc epsilon receptor I and stem cell factor receptor is differentially regulated by phosphatidylinositol 3-kinase and calcineurin in mouse bone marrow-derived mast cells. J. Immunol. **162:**2087–2094.
27. **Ishizuka, T., F. Okajima, M. Ishiwara, K. Iizuka, I. Ichimonji, T. Kawata, H. Tsukagoshi, K. Dobashi, T. Nakazawa, and M. Mori.** 2001. Sensitized mast cells migrate toward the antigen: a response regulated by p38 mitogen-activated protein kinase and Rho-associated coiled-coil-forming protein kinase. J. Immunol. **167:**2298–2304.
28. **Jabril-Cuenod, B., C. Zhang, A. M. Scharenberg, R. Paolini, R. Numerof, M. A. Beaven, and J. P. Kinet.** 1996. Syk-dependent phosphorylation of Shc. A potential link between FcepsilonRI and the Ras/mitogen-activated protein kinase signaling pathway through SOS and Grb2. J. Biol. Chem. **271:**16268–16272.
29. **Jersmann, H. P., C. S. Hii, J. V. Ferrante, and A. Ferrante.** 2001. Bacterial lipopolysaccharide and tumor necrosis factor alpha synergistically increase expression of human endothelial adhesion molecules through activation of NF-κB and p38 mitogen-activated protein kinase signaling pathways. Infect. Immun. **69:**1273–1279.
30. **Kalesnikoff, J., M. Huber, V. Lam, J. E. Damen, J. Zhang, R. P. Siraganian, and G. Krystal.** 2001. Monomeric IgE stimulates signaling pathways in mast cells that lead to cytokine production and cell survival. Immunity **14:**801–811.
31. **Kapus, A., C. Di Ciano, J. Sun, X. Zhan, L. Kim, T. W. Wong, and O. D. Rotstein.** 2000. Cell volume-dependent phosphorylation of proteins of the cortical cytoskeleton and cell-cell contact sites: the role of Fyn and FER kinases. J. Biol. Chem. **275:**32289–32298.
32. **Karasuyama, H., A. Rolink, and F. Melchers.** 1988. Recombinant interleukin 2 or 5, but not 3 or 4, induces maturation of resting mouse B lymphocytes and propagates proliferation of activated B cell blasts. J. Exp. Med. **167:**1377–1390.
33. **Kim, L., and T. W. Wong.** 1995. The cytoplasmic tyrosine kinase FER is associated with the catenin-like substrate pp120 and is activated by growth factors. Mol. Cell. Biol. **15:**4553–4561.
34. **Kim, L., and T. W. Wong.** 1998. Growth factor-dependent phosphorylation of the actin-binding protein cortactin is mediated by the cytoplasmic tyrosine kinase FER. J. Biol. Chem. **273:**23542–23548.
35. **Kitamura, D., H. Kaneko, Y. Miyagoe, T. Ariyasu, and T. Watanabe.** 1989. Isolation and characterization of a novel human gene expressed specifically in the cells of hematopoietic lineage. Nucleic Acids Res. **17:**9367–9379.
36. **Lee, S. H., M. Eom, S. J. Lee, S. Kim, H. J. Park, and D. Park.** 2001. BetaPix-enhanced p38 activation by Cdc42/Rac/PAK/MKK3/6-mediated pathway. Implication in the regulation of membrane ruffling. J. Biol. Chem. **276:**25066–25072.
37. **Li, H., T. C. Leung, S. Hoffman, J. Balsamo, and J. Lilien.** 2000. Coordinate regulation of cadherin and integrin function by the chondroitin sulfate proteoglycan neurocan. J. Cell Biol. **149:**1275–1288.
38. **Lilien, J., C. Arregui, H. Li, and J. Balsamo.** 1999. The juxtamembrane domain of cadherin regulates integrin-mediated adhesion and neurite outgrowth. J. Neurosci. Res. **58:**727–734.
39. **McCafferty, D. M., A. W. Craig, Y. A. Senis, and P. A. Greer.** 2002. Absence of Fer protein-tyrosine kinase exacerbates leukocyte recruitment in response to endotoxin. J. Immunol. **168:**4930–4935.
40. **Metcalfe, D. D., D. Baram, and Y. A. Mekori.** 1997. Mast cells. Physiol. Rev. **77:**1033–1079.
41. **Nishizumi, H., and T. Yamamoto.** 1997. Impaired tyrosine phosphorylation and Ca2+ mobilization, but not degranulation, in lyn-deficient bone marrow-derived mast cells. J. Immunol. **158:**2350–2355.
42. **Penhallow, R. C., K. Class, H. Sonoda, J. B. Bolen, and R. B. Rowley.** 1995. Temporal activation of nontransmembrane protein-tyrosine kinases following mast cell Fc epsilon RI engagement. J. Biol. Chem. **270:**23362–23365.
43. **Pivniouk, V. I., T. R. Martin, J. M. Lu-Kuo, H. R. Katz, H. C. Oettgen, and R. S. Geha.** 1999. SLP-76 deficiency impairs signaling via the high-affinity IgE receptor in mast cells. J. Clin. Investig. **103:**1737–1743.
44. **Razin, E., Z. Szallasi, M. G. Kazanietz, P. M. Blumberg, and J. Rivera.** 1994. Protein kinases C-beta and C-epsilon link the mast cell high-affinity receptor for IgE to the expression of c-fos and c-jun. Proc. Natl. Acad. Sci. USA **91:**7722–7726.
45. **Read, R. D., J. M. Lionberger, and T. E. Smithgall.** 1997. Oligomerization of the Fes tyrosine kinase. Evidence for a coiled-coil domain in the unique N-terminal region. J. Biol. Chem. **272:**18498–18503.
46. **Reth, M.** 1989. Antigen receptor tail clue. Nature **338:**383–384.
47. **Rosato, R., J. M. Veltmaat, J. Groffen, and N. Heisterkamp.** 1998. Involvement of the tyrosine kinase fer in cell adhesion. Mol. Cell. Biol. **18:**5762–5770.
48. **Scharenberg, A. M., S. Lin, B. Cuenod, H. Yamamura, and J. P. Kinet.** 1995. Reconstitution of interactions between tyrosine kinases and the high affinity IgE receptor which are controlled by receptor clustering. EMBO J. **14:**3385–3394.
49. **Schuuring, E., H. van Damme, E. Schuuring-Scholtes, E. Verhoeven, R. Michalides, E. Geelen, C. de Boer, H. Brok, V. van Buuren, and P. Kluin.** 1998. Characterization of the EMS1 gene and its product, human cortactin. Cell Adhes. Commun. **6:**185–209.
50. **Senis, Y., R. Zirngibl, J. McVeigh, A. Haman, T. Hoang, and P. A. Greer.** 1999. Targeted disruption of the murine fps/fes proto-oncogene reveals that Fps/Fes kinase activity is dispensable for hematopoiesis. Mol. Cell. Biol. **19:**7436–7446.
51. **Shirakabe, K., K. Yamaguchi, H. Shibuya, K. Irie, S. Matsuda, T. Moriguchi, Y. Gotoh, K. Matsumoto, and E. Nishida.** 1997. TAK1 mediates the ceramide signaling to stress-activated protein kinase/c-Jun N-terminal kinase. J. Biol. Chem. **272:**8141–8144.
52. **Smithgall, T. E., J. A. Rogers, K. L. Peters, J. Li, S. D. Briggs, J. M. Lionberger, H. Cheng, A. Shibata, B. Scholtz, S. Schreiner, and N. Dunham.**

1998. The c-Fes family of protein-tyrosine kinases. Crit. Rev. Oncog. **9:**43–62.
53. **Thompson, H. L., P. D. Burbelo, and D. D. Metcalfe.** 1990. Regulation of adhesion of mouse bone marrow-derived mast cells to laminin. J. Immunol. **145:**3425–3431.
54. **Thompson, H. L., L. Thomas, and D. D. Metcalfe.** 1993. Murine mast cells attach to and migrate on laminin-, fibronectin-, and matrigel-coated surfaces in response to Fc epsilon RI-mediated signals. Clin. Exp. Allergy **23:**270–275.
55. **Tian, L., D. L. Nelson, and D. M. Stewart.** 2000. Cdc42-interacting protein 4 mediates binding of the Wiskott-Aldrich syndrome protein to microtubules. J. Biol. Chem. **275:**7854–7861.
56. **Tibbles, L. A., Y. L. Ing, F. Kiefer, J. Chan, N. Iscove, J. R. Woodgett, and N. J. Lassam.** 1996. MLK-3 activates the SAPK/JNK and p38/RK pathways via SEK1 and MKK3/6. EMBO J. **15:**7026–7035.
57. **Tsai, M., L. S. Shih, G. F. Newlands, T. Takeishi, K. E. Langley, K. M. Zsebo, H. R. Miller, E. N. Geissler, and S. J. Galli.** 1991. The rat c-kit ligand, stem cell factor, induces the development of connective tissue-type and mucosal mast cells in vivo. Analysis by anatomical distribution, histochemistry, and protease phenotype. J. Exp. Med. **174:**125–131.
58. **Tsai, M., T. Takeishi, H. Thompson, K. E. Langley, K. M. Zsebo, D. D. Metcalfe, E. N. Geissler, and S. J. Galli.** 1991. Induction of mast cell proliferation, maturation, and heparin synthesis by the rat c-kit ligand, stem cell factor. Proc. Natl. Acad. Sci. USA **88:**6382–6386.
59. **Ueda, S., M. Mizuki, H. Ikeda, T. Tsujimura, I. Matsumura, K. Nakano, H. Daino, Z. Honda Zi, J. Sonoyama, H. Shibayama, H. Sugahara, T. Machii, and Y. Kanakura.** 2002. Critical roles of c-Kit tyrosine residues 567 and 719 in stem cell factor-induced chemotaxis: contribution of src family kinase and PI3-kinase on calcium mobilization and cell migration. Blood **99:**3342–3349.
60. **Vonakis, B. M., H. Haleem-Smith, P. Benjamin, and H. Metzger.** 2001. Interaction between the unphosphorylated receptor with high affinity for IgE and Lyn kinase. J. Biol. Chem. **276:**1041–1050.
61. **Watson, S. P., N. Asazuma, B. Atkinson, O. Berlanga, D. Best, R. Bobe, G. Jarvis, S. Marshall, D. Snell, M. Stafford, D. Tulasne, J. Wilde, P. Wonerow, and J. Frampton.** 2001. The role of ITAM- and ITIM-coupled receptors in platelet activation by collagen. Thromb. Haemostasis **86:**276–288.
62. **Wedemeyer, J., M. Tsai, and S. J. Galli.** 2000. Roles of mast cells and basophils in innate and acquired immunity. Curr. Opin. Immunol. **12:**624–631.
63. **Whitmarsh, A. J., and R. J. Davis.** 1996. Transcription factor AP-1 regulation by mitogen-activated protein kinase signal transduction pathways. J. Mol. Med. **74:**589–607.
64. **Yang, F. C., R. Kapur, A. J. King, W. Tao, C. Kim, J. Borneo, R. Breese, M. Marshall, M. C. Dinauer, and D. A. Williams.** 2000. Rac2 stimulates Akt activation affecting BAD/Bcl-XL expression while mediating survival and actin function in primary mast cells. Immunity **12:**557–568.
65. **Zirngibl, R., D. Schulze, S. E. Mirski, S. P. Cole, and P. A. Greer.** 2001. Subcellular localization analysis of the closely related Fps/Fes and Fer protein-tyrosine kinases suggests a distinct role for Fps/Fes in vesicular trafficking. Exp. Cell Res. **266:**87–94.